EXPERIMENTAL STUDY OF FLOW FIELD OF AN AEROFOIL SHAPED DIFFUSER WITH A POROUS SCREEN SIMULATING THE ROTOR

J. TANG, F. AVALLONE & G.J.W. VAN BUSSEL
Wind Energy Research Group, Faculty of Aerospace Engineering, Delft University of Technology, The Netherlands.

ABSTRACT

This study presents an experimental investigation on a diffuser augmented wind turbine (DAWT). A screen mesh is used to simulate the energy extraction mechanisms of a wind turbine in experiment. Different screen porosities corresponding to different turbine loading coefficients are tested. Measurements of the axial force and of the velocity distribution in radial direction are reported. The general purpose is to highlight the dependency between the diffuser and the screen, and to compare the radial velocity distributions in the diffuser between unloaded and loaded conditions. It is shown that the thrust on an unshrouded screen is lower than on a shrouded screen, under the same inflow condition. Moreover, the thrust on the diffuser largely depends on the screen loading. For the present configuration, the thrust on the screen with high loading coefficient contributes for more than 70% of the total thrust on the DAWT. Smoke visualizations and radial velocity profiles reveal that the high loading screen induces flow separation on the outer surface of the diffuser, justifying the results of the thrust measurements. It is also inferred that the flow separation leads to loss of thrust and has a great effect on the total pressure drag. It should be emphasized that the experimental results indicate that the flow field around the diffuser is strongly affected by the choice of screen porosity, that is, turbine loading. And that, the thrust coefficient of the diffuser does not show a linear dependence on the thrust coefficient of the screen. The axial momentum theory, therefore, is not a solid predictor for DAWT performance with high loaded screens.
Keywords: actuator disc, axial momentum theory, diffuser, ducted wind turbine.

1 INTRODUCTION

Thrust on horizontal axis wind turbines (HAWTs) is directly related to the pressure drop generated by rotating blades. The extracted power is given by the product of the mass flow through the rotor and the pressure drop across it. However, the total power that can be extracted is limited by the Betz limit. In order to increase the thrust, a higher pressure drop needs to be realized, but, as a consequence, the mass flow through the rotor reduces. According to Betz the optimal condition is a mass flow equal to 2/3rd of the original mass flow, from which 8/9th of the kinetic energy can be extracted.

The power of a wind turbine can be augmented by increasing the mass flow through the turbine. It has been shown that the application of a force perpendicular to the incoming wind results in an increase of mass flow. For HAWTs, this force can be realized by placing an annular lifting device around the rotor with its suction side pointing to the centre [1]. This annular lifting device can be a duct, a shroud or a diffuser with an aerofoil shaped cross-section. This is the principle behind a diffuser augmented wind turbine (DAWT), sometimes known as shrouded wind turbine or ducted wind turbine.

Various aspects of the DAWT have been investigated in the literature [2–9]. The boundary layer control solutions to a diffuser, mainly based on the blowing and swirling of the boundary layer are provided in [2–5]. Igra tested various diffuser geometries, including flaps and slots, finding, for the best configuration, an augmentation factor approximately three times

ISSN: 2046-0546 (paper format), ISSN: 2046-0554 (online), http://www.witpress.com/journals
DOI: 10.2495/CMEM-V4-N4-502-512

higher than a bare wind turbine with the same rotor diameter [6–8]. Abe *et al*. and Ohya *et al*. worked on shrouded wind turbine with the addition of a flange at the trailing edge and, they reported augmentation of power compared to bare wind turbine, in both field tests and wind tunnel experiments [10, 11].

Many analytical and computational approaches have been also proposed in the literature. Fletcher studied this topic with a computational method by combing his momentum theory and the Blade Element Method. He took the influence of the diffuser into account by introducing empirical values of the diffuser efficiency and of the exit-plane pressure coefficient. Good agreement was obtained both for power coefficient and turbine axial velocity with experimental results [9]. However, it was debatable to his experimental results as it were hampered by a very large blockage of the model.

Further studies based on wind tunnel experiments and axial momentum theory were performed subsequently. Hansen *et al*. found that the ratio between the mass flow through a ducted wind turbine and that through a bare turbine decreases by increasing the turbine thrust coefficient [12]. The analytical approach proposed by Van Bussel, in which he introduced the back pressure velocity ratio, pointed out that a power coefficient beyond the Betz limit cannot be achieved when the reference area is taken as the diffuser exit area [13]. Recently, Bontempo and Manna investigated the effects of the duct thrust on the power extraction from a DAWT, by means of a semi-analytical method [10]. They showed that the power output increases by increasing the duct thrust. However, this theoretical model was only compared with a numerical simulation.

To the knowledge of the authors, there is a lack of understanding of the aerodynamic interaction between the diffuser and the rotor. Its comprehension may lead to a better description of the phenomena and can give fundamental hints for developing future analytical models. Hence, in this work a DAWT is experimentally investigated. The rotor is simulated by actuator disc (AD) with two different porosities in order to produce two different turbine thrust coefficients. Measurements of the axial force and velocity distributions in the radial direction are reported.

2 DAWT THEORY

As stated in the introduction, the presence of a diffuser around a wind turbine increases the mass flow through the rotor and thus the power. In unloaded conditions, that is using an empty diffuser, the aerofoil-shaped diffuser generates an inward lift force that increases the mass flow through the diffuser. When incorporating an energy-absorbing wind turbine rotor, the axial momentum changes. This momentum change should be equal to the resultant axial force on the combined screen and diffuser. In the present study, the axial force exerted by the turbine, which is replaced by a screen simulator, is denoted by F_{screen} and the axial force on the diffuser by $F_{diffuser}$.

The pressure drop across the screen is assumed to be constant so that the 1D approximation can be applied. The F_{screen} is directly related to the pressure jump across the screen, while the $F_{diffuser}$ has various expressions. According to theory, $F_{diffuser}$ is linearly related to the pressure jump across the screen [1, 11, 14] provide a detailed discussion on the relationship between this pressure jump $C_{T,diffuser}$ and the circulation of the ring aerofoil.

Applying the axial momentum balance on the integrated DAWT:

$$F_{DAWT} = F_{diffuser} + F_{screen} = \rho V_1 A_{screen} \left(V_o - V_e \right) \tag{1}$$

Where V_1 is the (axial) velocity through the screen, V_0 is the wind speed, V_e is the velocity at diffuser exit and A_{screen} is the screen area (Fig. 1). Then the thrust coefficient is:

$$C_{T,DAWT} = \frac{\rho \mathrm{V}_1 A_{screen}\left(\mathrm{V}_\mathrm{o} - \mathrm{V}_\mathrm{e}\right)}{\frac{1}{2}\rho V_0^2 A_{screen}} = \frac{2\mathrm{V}_1\left(\mathrm{V}_\mathrm{o} - \mathrm{V}_\mathrm{e}\right)}{V_0^2} \tag{2}$$

The screen trust coefficient and diffuser thrust coefficient are defined as,

$$F_{screen} = \frac{1}{2}\rho V_0^2 A_{screen} C_{T,screen} \tag{3}$$

$$F_{diffuser} = \frac{1}{2}\rho V_0^2 A_{screen} C_{T,diffuser} \tag{4}$$

The ratio of thrust as thrust on diffuser and screen f then equal to,

$$f = \frac{F_{diffuser}}{F_{screen}} = \frac{C_{T,diffuser}}{C_{T,screen}} \tag{5}$$

Combining eqn (5) with eqn (1) leads to:

$$\left(1+f\right) C_{T,screen} = 2\frac{\mathrm{V}_1}{\mathrm{V}_\mathrm{o}}\left(1 - \frac{\mathrm{V}_\mathrm{e}}{\mathrm{V}_\mathrm{o}}\right) \tag{6}$$

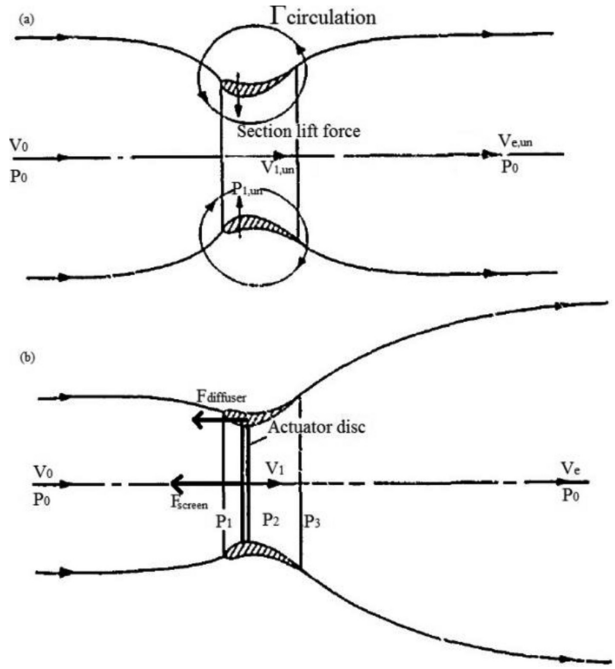

Figure 1: Aerofoil-shaped diffuser in inviscid flow, unloaded (a) and loaded condition (b) [1].

Hence, the normalized velocity at screen plane can be obtained by:

$$\frac{V_1}{V_o} = \frac{1+f}{2}\left(1+\frac{V_e}{V_o}\right) = \frac{1+f}{2}(1+\sqrt{1-C_{T,screen}}) \tag{7}$$

Using the Bernoulli equation as well as from DAWT theory [13], the thrust on rotor inside diffuser is assumed to be the same as the thrust on a bare wind turbine,

$$C_{T,screen} = 1-\left(\frac{V_e}{V_o}\right)^2 = 4a(1-a) \tag{8}$$

Van Bussel defined a back pressure velocity ratio (γ) at the diffuser exit area, specifying that a wake divergence downstream is possible in case the pressure at the diffuser exit has yet, not recovered to ambient pressure [13],

$$\gamma = v_3 / v_0 \tag{9}$$

$$C_{T,DAWT} = \beta\gamma 4a(1-a) \tag{10}$$

where β is the diffuser area ratio. The expression of thrust ratio can then directly be derived by

$$f = \beta\gamma - 1 \tag{11}$$

Based on eqn (10), the thrust on a diffuser is linearly dependent on the thrust on screen, and the coefficient value is related to the diffuser area ratio and back pressure velocity ratio. Since β is a fixed value for a specific diffuser, the mutual interaction between diffuser and screen, and hence *f,* is largely dependent on the back pressure it creates.

3 EXPERIMENT SETUP

The present study aims at providing an experimental analysis of the flow field of a diffuser and a screen emulating the rotor. Descriptions about the wind tunnel characteristics, the experimental setup and DAWT model are presented in this section.

3.1 Wind tunnel setup

The experiment is conducted in the closed loop open-jet wind-tunnel of the faculty of Aerospace Engineering of Delft University of Technology. The wind tunnel has an octagonal nozzle with a 3 m equivalent diameter and settling chamber with a contraction ratio of 3:1. The free-stream flow at the measurement location has a turbulence intensity of 0.2%, and the flow temperature is kept constant at 20℃ by a heat exchanger. The wind tunnel is operated at free-stream velocity ranging between 5 m/s and 10 m/s. Based on the specifications provided by the manufacturer, the DAWT has the cut-in wind speed at 4 m/s and has the output wind speed at 14 m/s, but the axial load on duct at 14 m/s is beyond the balance limit, thus choosing the wind speed ranges from 5 m/s to 10 m/s.

3.2 Diffuser model

The experimentally investigated DAWT model is composed as follows: the diffuser is taken from the commercial *donQi Urban Windmill* 1.5, while the rotor is simulated using an actuator disc (AD) [15]. The diffuser model has an area ratio (β) equal to 1.73. The exit plane of

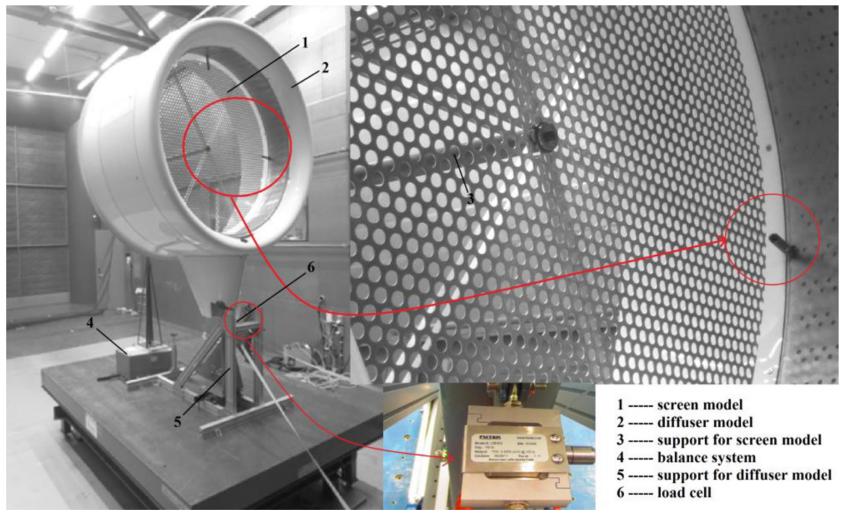

Figure 2: Screen model combined with diffuser model (test 1).

the diffuser has a diameter of 2 m and is equipped with a Gurney flap 40 mm long intended to an increase the performance of the DAWT.

The AD is realized using a perforated screen. Two screens with different porosities are investigated. The porosity (p) is a measure of the permeability of the area of the screen and it is defined as the ratio between the open area and the total area of the screen. The two screens have porosities equal to $p = 40\%$ and $p = 46\%$, thus resulting in thrust coefficients $C_{T,screen}$ equal to 0.92 and 0.87, respectively.

The diffuser is set parallel to the flow, at 0° yaw angle. It is installed on a support equipped with a load cell (Model: LSB302 from *FUTEK*), while the screen is installed on a separate structure connected with a six-component balance system. This experimental setup is shown in Fig. 2.

3.3 Axial force measurements

The measurements of the thrust at different wind speeds ranging between 5 m/s and 10 m/s are carried out using a six-component balance system and a load cell. The accuracy of the balance system is ±0.23% of the measured load, the reference system of balance is shown in Fig. 3.

In order to check the quality and repeatability of the measurements, two different configurations are carried out. In test 1, the screen and the diffuser are mounted independently and thrust forces are measured by means of the balance system and load cell respectively. In test 2, the screen is physically connected with the diffuser and the total thrust is measured by using the load cell.

3.4 Velocity field configuration

Velocity measurements with a pitot probe are carried out along the radial directions for both the unloaded and loaded diffuser. For each measurement, data are averaged over a sequence of 10 s. Radial measurements are performed at $x/L = 30$ mm (i.e. 3 cm in front of the screen

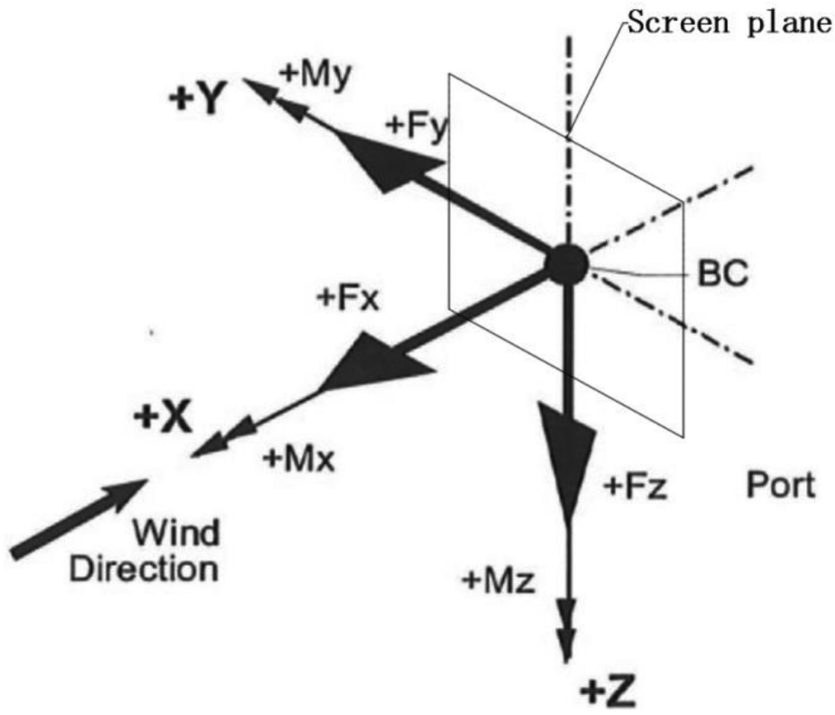

Figure 3: Reference system for balance system.

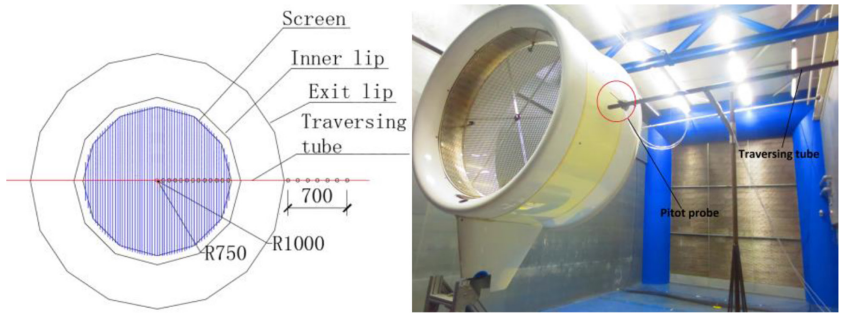

Figure 4: Schematics representing the velocity measurements setup.

plane), where L is the diffuser length equal to 1 m in the range $0<r/R<1$ and $1.12<r/R<1.94$ (here R refers to screen radius and equals to 750 mm).

4 RESULTS AND DISCUSSION

4.1 Thrust measurements

In this section thrust measurements of the investigated configurations are reported and discussed. Comparisons of the different configurations are shown in Fig. 5.

Figure 5 reports both the $C_{T,diffuser}$ and $C_{T,screen}$ at five different V_0. According to the DAWT theory, the thrust on the screen located inside a diffuser is the same as the thrust on a bare

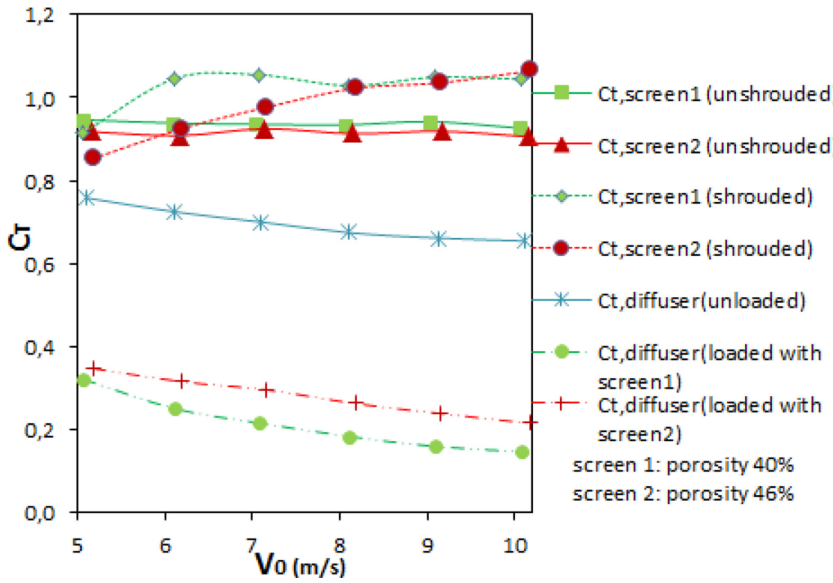

Figure 5: Thrust coefficient varying the free-stream velocity.

screen [13]. However, Fig. 5 shows that the thrust on a shrouded screen, is greater than on the unshrouded screen contrary to what is expected from the DAWT theory. The increase of shrouded $C_{T,screen}$ compared to unshrouded $C_{T,screen}$ varies from 5% to 18%. By enclosing a diffuser, the aerodynamic interaction between the diffuser and screen increases the thrust on the screen.

With the presence of the screen, the $C_{T,diffuser}$ reduces by about 50%, compared to the unloaded $C_{T,diffuser}$. According to the analytical solution reported in eqn (11), the $C_{T,diffuser}$ is assumed to increase with higher $C_{T,screen}$. However, data show that when the bare $C_{T,screen}$, is higher than the optimal Betz coefficient ($C_{T,screen} > 0.89$), the $C_{T,diffuser}$ decreases when increasing $C_{T,screen}$. It is inferred that the relationship between $C_{T,diffuser}$ and $C_{T,screen}$ is not linear; particularly, the screen loading coefficient is beyond 0.89.

Moreover, it is noted that by increasing V_0, the variation of $C_{T,screen}$ between shrouded and unshrouded conditions increases. The mutual interaction between diffuser and high loaded screen causes these discrepancies, especially with a high loading screen.

Figure 6 compares the result of thrust measurements between the two test runs: one with screen unconnected with the diffuser and the other connected with it. The dashed lines in Fig. 6, are the results of test 1, obtained as the sum of separately measured thrust on screen and diffuser. The solid lines are the direct measurement results of the integrated screen and diffuser configuration (test 2). For the higher disc loading (screen 1 with $C_{T,screen} = 0.92$), both curves slightly decrease with the increasing V_0. Differently, for the lower disc loading (screen 2 with $C_{T,screen} = 0.87$), the thrust coefficient increases with V_0. The discrepancies behind this behaviour will be further investigated in the future.

Combing the results shown in Fig. 5, the screen greatly contributes to the overall thrust coefficient. The thrust on screen, when it has a high loading coefficient, contributes over 70% on the total thrust on the DAWT. This means that the performance of screen have the dominant effect on the total thrust.

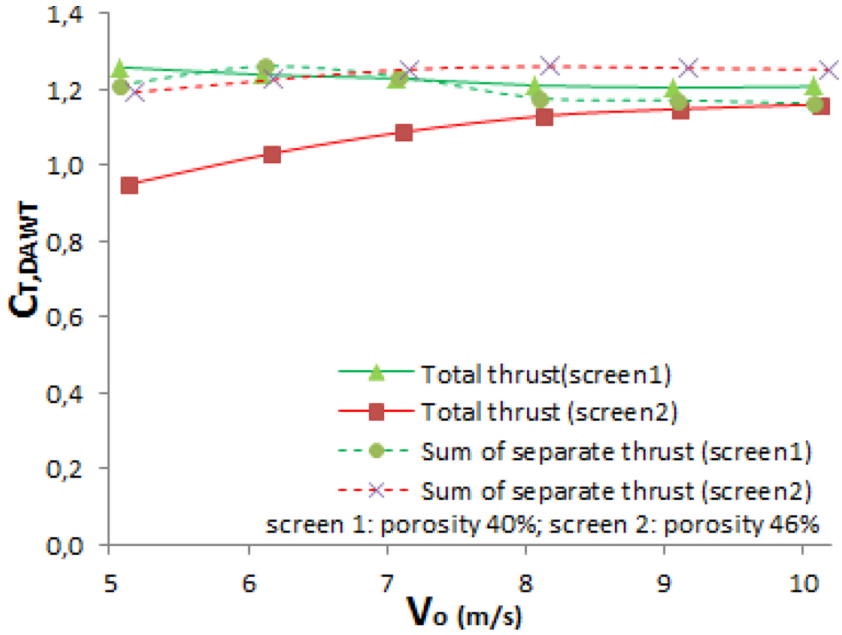

Figure 6: Comparison between measurements of the total thrust measured with the load cell and the thrust obtained by summing the two different contributions (i.e. force measured separately on the diffuser and on the screen).

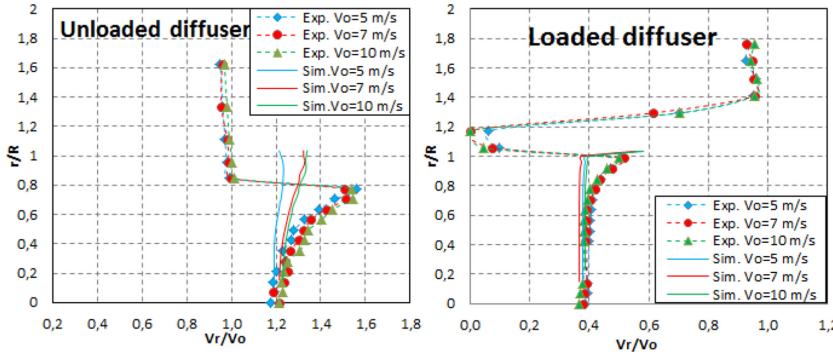

Figure 7: Velocity distribution at screen plane in different diffuser loading.

4.2 Global velocity field in unloaded diffuser and loaded diffuser

The results are taken at the lower half of the domain considering the symmetry of the flow. The increase in velocity inside the diffuser is observed as expected from the DAWT theory. The left plot of Fig. 7 presents the radial velocity profile for the unloaded diffuser ($C_{T,screen}$ = 0); it is evident that the velocity recovers to free-stream velocity in the diffuser external area (near the inner wall). The further away from the diffuser, the lower the velocity. This means that there is no flow separation in this zone. Differently, in the right plot it is shown that in the presence of the high loading screen ($C_{T,screen}$ = 0.92), the velocity ratio drops to zero at 1<*r/R*<1.2. The hypothesis therefore is made that flow separation is present in this

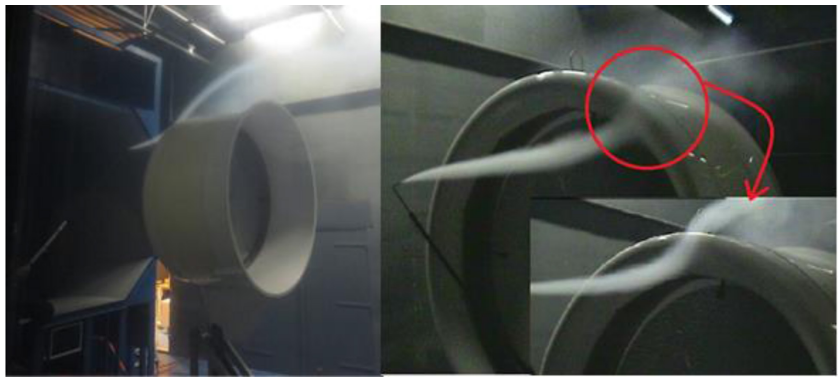

Figure 8: Smoke visualization around diffuser outer surface from inlet to exit.

zone. To summarize, the radial velocity profile justifies the results obtained from the thrust measurements.

The experimental data is consistent with the simulation results [16]. The small differences between experiment data and numerical calculation may, amongst others, be explained by the small wind tunnel blockage effect. The correction to dynamic pressure is 0.96, which means that the incoming velocities have to be corrected with a factor equal to the square root of 0.96. It should be stressed that all the experiment data present in this study have been corrected for.

4.3 Smoke visualization

For an unloaded diffuser, the flow around its inner surface and outer surface is quite fluent whereas, with the presence of high loading screen (screen 1 with $C_{T,screen} = 0.92$), flow separation is present on the outer surface of diffuser as can be seen in Fig. 8. This means that the separation is not related to the wind tunnel blockage effect. The flow separation starts from the leading edge and is fully developed subsequently. Hence, a low velocity atmospheric pressure region along the diffuser external contour builds up. This creates less lift and thereby a smaller core flow, which in its turn results in less mass flow passing through diffuser. It is inferred that the mass flow in an unloaded diffuser is more than the diffuser with a high loading screen.

It is noted that on the loaded diffuser suction-side, the flow is non-separated. Separation is not predicted in the 2D computations based on this configuration, probably due to the use of the k-ωSST turbulence model together with wall functions on the diffuser surfaces.

5 CONCLUSIONS

The study presents an experimental analysis of the variation of axial force on DAWT and its velocity distribution. The axial force on the diffuser largely depends on the screen loading. Considering the total thrust on DAWT, the thrust on screen, when it has a high loading, contributes to over 70% of the total thrust on the DAWT. And that the thrust on the unshrouded screen is greater than on the shrouded screen, under the same ambient (wind tunnel) velocity.

In the presence of the high loading screen, separation occurs on the diffuser outer surface, which leads to loss of diffuser lift and, hence, thrust and this has a great effect on the total pressure drag. The separation is believed to be mainly caused by the high loading of the screen, which has a thrust coefficient considerably greater than the theoretical Betz limit value ($C_{T,screen} = 0.89$).

The velocity profiles are measured under the condition of unloaded diffuser and loaded diffuser with the porous screen. In general, the experimental data of normalized velocities at screen plane is consistent with the simulation results. The differences between experimental data and numerical calculation may be explained by the small wind tunnel blockage effect.

Meanwhile, the velocity distribution in radial direction and smoke visualization showed that the high loading screen induces a flow separation on the outer surface of the diffuser. This justified the results obtained by the thrust measurements.

The thrust experienced by a diffuser is directly affected by the turbine loading. However, the thrust coefficient of a diffuser is not linearly dependent on the thrust coefficient of screen. As a consequence, axial momentum theory is not a solid predictor for DAWT performance with high loaded screens.

ACKNOWLEDGEMENTS

Vinit Dighe, Nikolaos C. Antsos, Nando Timmer and Nico van Beek are thanked for their substantial support for this work. Financial support provided by the STW organization (grant number-12728) from the Netherlands and the CSC Scholarship from the Chinese government is gratefully acknowledged.

REFERENCES

[1] de Vries, O., *Fluid Dynamic Aspects of Wind Energy Conversion*, 1979.

[2] Gilbert, B.L. & Foreman, K.M., Experiments with a diffuser-augmented model wind turbine. *Journal of Energy Resource Technology*, **105**(1), pp. 46–53, 1983. http://dx.doi.org/10.1115/1.3230875

[3] Foreman, K., Preliminary design and economic investigations of Diffuser Augmented Wind Turbines (DAWT). *Final Report, 15 May 1979-31 Mar. 1980*, 1981. http://dx.doi.org/10.1016/0038-092X(78)90122-6

[4] Foreman, K.M., Gilbert, B. & Oman, R.A., Diffuser augmentation of wind turbines. *Solar Energy*, **20**, pp. 305–311, 1978.

[5] Foreman, K.M. & Gilbert, B.L., Further investigations of diffuser augmented wind turbines part II, 1979.

[6] Igra, O., Design and performance of a turbine suitable for an aerogenerator. *Energy Convers*, **15**(3–4), pp. 143–151, 1976. http://dx.doi.org/10.1016/0013-7480(76)90026-7

[7] Igra, O., The shrouded aerogenerator. *Energy*, **2**(4), pp. 429–439, 1977. http://dx.doi.org/10.1016/0360-5442(77)90006-8

[8] Igra, O., Research and development for shrouded wind turbines. *Energy Conversion Management*, **21**(1), pp. 13–48, 1981. http://dx.doi.org/10.1016/0196-8904(81)90005-4

[9] Fletcher, C.A.J., Computational analysis of diffuser-augmented wind turbines. *Energy Conversion and Management*, **21**(3), pp. 175–183, 1981. http://dx.doi.org/10.1016/0196-8904(81)90012-1

[10] Bontempo, R. & Manna, M., Effects of the duct thrust on the performance of ducted wind turbines. *Energy*, **99**, pp. 274–287, 2016. http://dx.doi.org/10.1016/j.energy.2016.01.025

[11] Werle, J., Shroud and ejector augmenters for subsonic propulsion & power systems. *Journal of Propulsion and Power*, **25**(1), pp. 228–236, 2009. http://dx.doi.org/10.2514/1.36042

[12] Hansen, M.O.L., Sørensen, N.N. & Flay, R.G.J., Effect of placing a diffuser around a wind turbine. *Wind Energy*, **3**(4), pp. 207–213, 2000.
http://dx.doi.org/10.1002/we.37

[13] Van Bussel, G.J.W., The science of making more torque from wind: Diffuser experiments and theory revisited. *Journal of Physics: Conference Series*, **75**, p. 012010, 2007.
http://dx.doi.org/10.1088/1742-6596/75/1/012010

[14] Werle, M.J. & Presz, W.M., Ducted wind/water turbines and propellers revisited. *Journal of Propulsion and Power*, **24**(5), pp. 1146–1150, 2008.
http://dx.doi.org/10.2514/1.37134

[15] Lignarolo, L.E.M., Ragni, D., Krishnaswami, C., Chen, Q., Simão Ferreira, C.J. & van Bussel, G.J.W., Experimental analysis of the wake of a horizontal-axis wind-turbine model. *Renewable Energy*, **70**, pp. 31–46, 2014.
http://dx.doi.org/10.1016/j.renene.2014.01.020

[16] Dighe, V.V., Avallone, F. & van Bussel, G.J.W., Computational study of diffuser augmented wind turbine using actuator disc force method. In *AFM2016 11th International Conference on Advances in Fluid Mechanics*, p. 12, 2016.

[17] Igra, O., Compact shrouds for wind turbines. *Energy Conversion*, **16**(4), pp. 149–157, 1977.
http://dx.doi.org/10.1016/0013-7480(77)90022-5